HHS Public Access

Author manuscript

J Autoimmun. Author manuscript; available in PMC 2019 December 01.

Published in final edited form as:

J Autoimmun. 2018 December ; 95: 47–57. doi:10.1016/j.jaut.2018.09.010.

Gut Microbiota Translocation Promotes Autoimmune Cholangitis

Hong-Di Ma[1,2,3], **Zhi-Bin Zhao**[1,2,3], **Wen-Tao Ma**[3], **Qing-Zhi Liu**[1,2,3], **Cai-Yue Gao**[1,2,3], **Liang Li**[1,2,3], **Jinjun Wang**[4], **Koichi Tsuneyama**[5], **Bin Liu**[6], **Weici Zhang**[7], **Yongjian Zhou**[1,*], **M. Eric Gershwin**[7], and **Zhe-Xiong Lian**[1,2,3,*]

[1]Department of Gastroenterology, Guangzhou Digestive Disease Center, Guangzhou First People's Hospital, School of Medicine, South China University of Technology, Guangzhou, Guangdong, 510180, China

[2]Chronic Disease Laboratory, Institutes for Life Sciences and School of Medicine, South China University of Technology, Guangzhou 510006, China

[3]Liver Immunology Laboratory, The CAS Key Laboratory of Innate Immunity and Chronic Disease, School of Life Sciences, University of Science and Technology of China, Hefei, Anhui, China

[4]College of Environmental Science and Engineering, Yangzhou University, Yangzhou 225127, Jiangsu Province, Chin

[5]Department of Molecular and Environmental Pathology, Institute of Health Biosciences, The University of Tokushima Graduate School, Tokushima, Japan

[6]Department of Rheumatology and Immunology, the Affiliated Hospital of Qingdao University, Qingdao, China

[7]Division of Rheumatology, Allergy and Clinical Immunology, University of California at Davis School of Medicine, Davis, CA, USA

Abstract

Gut microbiota and bacterial translocation have been implicated as significant contributors to mucosal immune responses and tolerance; alteration of microbial molecules, termed pathogen-associated molecular patterns (PAMP) and bacterial translocation are associated with immune pathology. However, the mechanisms by which dysregulated gut microbiota promotes autoimmunity is unclear. We have taken advantage of a well-characterized murine model of primary biliary cholangitis, dnTGFβRII mice, and an additional unique construct, toll-like receptor 2 (TLR2)-deficient dnTGFβRII mice coined dnTGFβRIITLR2$^{-/-}$ mice to investigate the

[*]**Correspondence to**: Zhe-Xiong Lian, M.D., Ph.D., Chronic Disease Laboratory, Institutes for Life Sciences and School of Medicine, South China University of Technology, Guangzhou 510006, China; Phone: +86-20-39380962; zxlian@scut.edu.cn or Yongjian Zhou, yizhou@gzhmu.edu.cn.

Author contributions:

Hong-Di Ma, Yongjian Zhou, M. Eric Gershwin, and Zhe-Xiong Lian designed the experiments and wrote the paper. Hong-Di Ma carried out most of the experimental work and analyzed data. Zhi-Bin Zhao, Wen-Tao Ma, Qing-Zhi Liu, Cai-Yue Gao, Liang Li, Jinjun Wang, Weici Zhang and Bin Liu contributed to some experiments. Koichi Tsuneyama conducted the pathological analysis.

Conflict of interest: None.

influences of gut microbiota on autoimmune cholangitis. Firstly, we report that dnTGFβRII mice manifest altered composition of gut microbiota and that alteration of this gut microbiota by administration of antibiotics significantly alleviates T-cell-mediated infiltration and bile duct damage. Second, toll-like receptor 2 (TLR2)-deficient dnTGFβRII mice demonstrate significant exacerbation of autoimmune cholangitis when their epithelial barrier integrity was disrupted. Further, TLR2-deficiency mediates downregulated expression of tight junction- associated protein ZO-1 leading to increased gut permeability and bacterial translocation from gut to liver; use of antibiotics reduces microbiota translocation to liver and also decreases biliary pathology. In conclusion, our data demonstrates the important role of gut microbiota and bacterial translocation in the pathogenesis of murine autoimmune cholangitis.

Keywords

primary biliary cholangitis; gut microbiota; fecal bacterial analysis; bacterial translocation; gut-liver axis

1. Introduction

Primary biliary cholangitis (PBC) [1] is characterized by the presence of anti-mitochondrial antibodies (AMA), infiltration of inflammatory lymphocytes, and destruction of intrahepatic small bile ducts. Epidemiological studies have reported that preceding bacterial infections, especially *Escherichia coli (E. coli),* correlates with an increased risk of developing PBC [2, 3]. Analysis of human PBC liver using 16S rRNA sequencing, reveals that *Propionibacterium acnes* is involved in granuloma formation [4]. Altered gut microbial profile has been reported in patients with PBC and is partially restored after ursodeoxycholic acid (UDCA) therapy [5].

The liver has a unique anatomy and is at the junction of a hemodynamic confluence, thereby receiving blood from both the systemic circulation and intestine [6]. Food-derived antigens and pathogen-associated molecular patterns (PAMPs) derived from intestinal bacteria flow into the liver through the portal vein [7]. Other connections between the gut and liver include transfer of PAMPs and potential bacterial translocation [8–10]. The constant exposure to stimuli from gut contributes to a distinctive local immune environment in the liver [11]. Although the liver maintains tolerance [12], increasing evidence demonstrates that tolerance can be reversed by intestinal dysbiosis, as reflected in several diseases including liver fibrosis [13], cirrhosis [14], non-alcoholic fatty liver disease [15], autoimmune hepatitis[16], primary sclerosing cholangitis (PSC) [17, 18], and PBC [5].

In this report, toll-like receptors (TLRs) are important components of the gut-liver axis [9].TLRs can not only recognize bacterial antigens transported through the portal vein but also participate in maintaining integrity of the intestinal epithelial barrier [19, 20]. Given the importance of TLR2 in maintaining tight-junctions [19], herein using dnTGFβRII mice, TLR2-deficient dnTGFβRII mice and TLR4-deficient dnTGFβRII mice, we report a potentially important mechanism; a defective intestinal tight junction barrier due to TLR2-deficiency, is critical for mediating hepatic inflammation and tissue damage by facilitating gut bacterial translocation to liver.

2. Materials and methods

2.1 Mice

dnTGFβRII (TG) mice with a C57BL/6 background (B6.Cg-Tg(Cd4-TGFBR2)16Flv/J) [21] were initially derived from stock from the from Jackson Laboratory (Bar Harbor, ME, USA). The maintenance and genetic monitoring of this colony has been previously reported [22]. TLR2 knockout mice also on a C57BL/6 background were kindly provided by Dr. Shao- Bo Su (Sun Yat-sen University, Guangzhou, Guangdong, China). dnTGFβRIITLR2−/− (TGT2) mice were obtained by selectively backcrossing dnTGFβRII mice with TLR2 knockout mice. Wide-type (WT) littermates were obtained by crossing dnTGFβRII mice with WT mice. All mice were housed in a specific pathogen-free and controlled environment (22 °C, 55% humidity, and 12-h day/night rhythm) and care was provided according to the regulations of animal care at the University of Science and Technology of China (Hefei, Anhui, China).

2.2 Animal protocol

We first used 16S rRNA sequencing to analyze fecal bacteria of 12–14-week-old female dnTGFβRII mice and their littermate B6 controls.

In order to evaluate the effects of gut microbiota on PBC murine model, antibiotics were fed to 12–14-week-old female dnTGFβRII mice (TG+ABx mice) to compare liver infiltration with control untreated dnTGFβRII mice (TG mice).

In order to prove that the disrupted epithelial barrier could increase hepatic inflammation and aggravate autoimmune liver disease, we examined the liver and colon inflammation and infiltration when intestinal barrier was broken in 12–14-week-old female dnTGFβRIITLR2−/− mice (TGT2 mice) compared with dnTGFβRII mice (TG mice). Similarly, antibiotics were used to treat 12–14-week-old female dnTGFβRIITLR2−/− mice (TGT2+ABx mice) to evaluate the effect of gut microbiota on the natural history of dnTGFβRIITLR2−/− mice, compared with untreated dnTGFβRIITLR2−/− mice (TGT2 mice). In addition, we also examined the liver and colon inflammation in 12–14-week-old female dnTGFβRIITLR4−/− mice (TGT4 mice) to detect the role of TLR4 in our PBC murine model.

2.3 Antibiotics treatment

The antibiotic regimen began by treating pregnant mothers of dnTGFβRII and dnTGFβRIITLR2−/− (TGT2) mice with a mixture of 1 mg/mL ampicillin, 1 mg/mL neomycin sulfate, and 1 mg/mL metronidazole, in drinking water. Three weeks after birth, the mice were moved to a new cage and treated with antibiotics until 12–14 weeks old, at which point they were used for experiments. The water containing the mixed antibiotics was changed twice a week.

2.4 Fecal bacterial analysis

Stool samples were collected from 12–14-week-old female dnTGFβRII mice and littermate B6 mice, snap-frozen, and stored at −80 °C until further use. Total DNA was then extracted

using the QIAamp DNA Stool Mini Kit (Qiagen, Hilden, Germany) and quantified [23]. The V3 region of the 16SrRNA gene was amplified and sequenced on a 454 Genome Sequencer FLX Titanium platform (Roche Diagnostics and Beckman Coulter Genomics) [24]. The sequencing data were submitted to the MG-RAST server and compared by phylum or family prevalence among groups [25, 26]. The sequences have been deposited to the GenBank Sequence Read Archive database (https://www.ncbi.nlm.nih.gov/sra) under accession numbers SRP123383.

2.5 Liver and colon tissue preparation and histological scoring

Liver and colon tissues from dnTGFβRII and dnTGFβRIITLR2−/− mice were fixed with 4% paraformaldehyde, dehydrated using graded ethanol, vitrified using dimethylbenzene, and embedded in paraffin. The liver tissues were cut into 4-μm sections and colon tissues into 6-pm sections and then deparaffinized, stained with hematoxylin and eosin (H&E), and evaluated using light microscopy. Histological scoring were carried out in a “blinded” manner by a pathologist (K.T.), as described previously [14, 27].

Firstly, the degree of portal inflammation was evaluated and scored according to the most severe lesions as follows: 0, no change; 1, minimal inflammation; 2, mild inflammation; 3, moderate inflammation; 4, severe inflammation. In addition, the degree of inflammatory frequency in a specimen was determined by the percentage of affected tissue within the total hepatic lobules per specimen and coded as follows: 0, none, 1, 1%−10%; 2, 11–20%; 3, 21–50%; 4, more than 50%. Finally, a summary score that includes severity and frequency analysis was generated as the sum of these scores.

Second, bile duct damage was evaluated firstly by the degree of severity in the most severe lesions as follows: 0, no change; 1, epithelial damage (only cytoplasmic change); 2, epithelial damage with cytoplasmic and nuclear change; 3, non-suppurative destructive cholangitis (CNSDC); 4, bile duct loss. The frequency of bile duct damage was then scored as follows: 0, none; 1, 1%−10%; 2, 11–20%; 3, 21–50%; 4, more than 50%. To obtain an integrative evaluation, the scores of severity and frequency were added together.

Third, colon histopathology was scored as follows: 0, no significant changes; 1, minimal scattered mucosal inflammatory cell infiltrates, with or without minimal epithelial hyperplasia; 2, mild scattered to diffuse inflammatory cell infiltrates, sometimes extending into the submucosa and associated with erosions, with mild to moderate epithelial hyperplasia and mild to moderate mucin depletion from goblet cells; 3, moderate inflammatory cell infiltrates that were sometimes transmural, with moderate to severe epithelial hyperplasia and mucin depletion; and 4, marked inflammatory cell infiltrates that were often transmural and associated with crypt abscesses and occasional ulceration, with marked epithelial hyperplasia, mucin depletion, and loss of intestinal glands.

2.6 Preparation of hepatic mononuclear cells and flow cytometric analysis

Hepatic mononuclear cells were isolated from the liver with the exception of using 40%/70% Percoll (GE Healthcare, Little Chalfont, United Kingdom) instead of Histopaque-1.077 [28]. Then, mononuclear cells were collected by centrifugation at 800 *g* for 5 min and counted. Cell preparations were first incubated with anti-mouse FcR blocking

reagent (Biolegend, San Diego, CA, US) and then stained with mixed fluorochrome-conjugated antibodies (Abs) at 4 °C in PBS with 0.2% bovine serum albumin for 20 min. All fluorochrome- conjugated Abs, unless otherwise noted, were purchased from Biolegend (San Diego, California, USA).

To detect hepatic mononuclear cell subsets and T cell subsets, hepatic mononuclear cells from mice were stained with PacificBlue-CD3 (17A2), APC-Cy7-CD8α (19517), V500-CD4 (RM4–5, BD Bioscience), APC-NK1.1 (PK136), PE/Cy7-CD19 (6D5), FITC-CD44 (IM7), and PerCP/Cy5.5-CD62L (MEL-14). Stained cells were analyzed using a FACSVerse flow cytometer (BD Immunocytometry Systems, San Jose, CA, USA). Flow data were calculated using the FlowJo software (Tree Star, Ashland, OR, US).

2.7 Immunofluorescence

Colon tissues from 12–14-week-old female wide type controls, dnTGFβRII, and dnTGFβRIITLR2−/− mice were fixed, dehydrated, and immersed in Tissue-Tek OCT compound (Sakura, Japan) [29]. Frozen colon tissues were cut into 8-μm sections. After blocking with homologous serum, the colon sections were incubated with anti-ZO-1 tight-junction protein primary antibody (ab59720, Abcam, Cambridge, MA, US), then detected with Alexa Fluor 647-goat anti-rabbit IgG(H+L) secondary antibody (A-21245, Invitrogen, Thermo Fisher Scientific), and stained with DAPI (AR1176, BOSTER, Wuhan, China). Images were visualized using confocal microscopy (LSM 710, Carl Zeiss).

2.8 Immunoblotting

Colon samples from 12–14-week-old female dnTGFβRII and dnTGFβRIITLR2−/− mice were homogenized [29]. Total proteins from the colon samples were separated by sodium dodecyl sulfate-polyacrylamide gel electrophoresis (SDS-PAGE) and transferred to polyvinylidene difluoride (PVDF) membranes (Millipore, Billerica, MA, USA). Proteins were detected by primary antibodies against ZO-1 tight junction protein (ab59720, abcam, Cambridge, MA, US) or GAPDH (Genesci, Shanghai, China), and HRP-labeled anti-rabbit secondary antibodies (Cell Signaling Technology, Boston, MA, US).

2.9 FITC-dextran intestinal permeability assay

Intestinal permeability was measured using 4,000-Da fluorescent dextran (Sigma-Aldrich, St. Louis, MO) [30]. Briefly, 12-h water-fasted wide type controls, dnTGFβRII, and dnTGFβRIITLR2−/− mice were administered with fluorescein isothiocyanate (FITC)-dextran by oral gavage (44 mg/100 g body weight, 100 mg/mL). After 4 h, blood was collected from the ophthalmic vein. Serum samples were obtained and analyzed for FITC-dextran concentration with a fluorescence spectrophotometer (Synergy2 Multi-Mode Reader, BioTek, Winooski, VT, USA).

2.10 Liver CFU measurement

Fresh livers isolated from 12–14-week-old female wide type controls, dnTGFβRII, and dnTGFβRIITLR2−/− mice as well as antibiotic-treated dnTGFβRIITLR2−/− mice were homogenized and plated on Columbia Blood Agar Base (Tianda Diagnostic Reagent Co.,

Ltd., Hefei, Anhui, China). Twenty-four hours after incubation, the CFUs were counted and calculated as count per gram weight of the liver.

2.11 Statistical analysis

All data are presented as the mean ± standard deviation (SD). The significance of differences was determined using a two-tailed unpaired Student's *t* test in GraphPad Prism. All experiments were replicated at least three times. The significance levels are denoted as $*p < 0.05$, $**p < 0.01$, $***p < 0.001$, as applicable.

3. Results

3.1 Dysbiosis of gut microbiota participates in the pathogenesis of T-cell-mediated cholangitis in dnTGFβRII mice

Fecal 16S rRNA sequencing analysis revealed altered gut microbiota composition in dnTGFβRII mice compared to WT controls. At the phylum level, the abundance of Firmicutes and Bacteroidetes was markedly altered. The relative proportion of Firmicutes increased from 21% to 52%, while that of Bacteroidetes decreased from 72% to 43% in dnTGFβRII mice compared with WT mice (Figure 1A). At the family level, we found a reduction in the proportion of S24–7, Ruminococcaceae, Rikenellaceae, and Porphyromonadaceae, and a marked increase in the proportion of Lachnospiraceae and Bacteroidaceae in dnTGFβRII mice compared with the WT controls (Figure 1B). Analysis of 16S ribosomal RNA (rRNA) sequencing from fecal samples also revealed a markedly diminished richness and diversity of the gut microbiota in dnTGFβRII mice compared to WT mice (Figure 1C).

Next, we treated dnTGFβRII mice with antibiotics (TG+ABx) to alter the gut microbiota and found that such treatment significantly reduced the number of liver mononuclear cells (MNCs) in dnTGFβRII mice (Figure 2A, $p < 0.001$). The number of liver T cells ($p < 0.001$), CD8+T ($p < 0.001$), and CD4+T ($p < 0.001$) cells significantly decreased after antibiotic treatment (Figure 2B). Notably, there was an obvious decrease of activated effector memory CD8+T (CD8Tem) (Figure 2C) and CD4+T (CD4Tem) (Figure 2D) cell subsets (CD44+CD62L-) both in terms of frequency (CD8Tem, $p = 0.0308$; CD4Tem, $p = 0.0179$) and number ($p < 0.001$) with antibiotic treatment.

3.2 Disrupted epithelial barrier exacerbates hepatic T-cell-mediated cholangitis in dnTGFβRII mice

Compared to age- and sex-matched dnTGFβRII (TG) mice, TLR2-knockout dnTGFβRII (TGT2) mice manifest severe cholangitis (Figure 3A), as reflected by increased scores of portal inflammation (Figure 3B, $p = 0.0011$) and bile duct damage (Figure 3C, $p = 0.0108$) and numbers of infiltrated liver MNCs (Figure 3D, $p = 0.0431$). Liver T cells in dnTGFβRIITLR2−/− mice were increased compared with dnTGFβRII mice (Figure 3E, $p = 0.0105$). Amongst the T cells, there was an increased number of CD4+T cells in dnTGFβRIITLR2−/− mice (Figure 3E, $p = 0.0075$), and they appeared to be more active than in dnTGFβRII mice, with a higher percentage ($p = 0.0054$) and total number ($p = 0.0074$) of effector memory (CD44+CD62L-) CD4+T cells in dnTGFβRIITLR2−/− mice

(Figure 3F). However, unlike in dnTGFβRIITLR2−/−, TLR4 deficiency had no effects on cholangitis and colitis (Figure S1, S2) in the PBC mouse model. Thus, a disrupted epithelial barrier seemed to increase hepatic inflammation and aggravate autoimmune liver disease.

3.3 TLR2 deficiency aggravated colitis and colon injury in dnTGFβRII mice

TLR2 deficiency also induced severe intestinal injury and inflammation in dnTGFβRII mice (Figure 4A). dnTGFβRII mice exhibited mild mucosal infiltration of immune cells in the colon (Figure 4A, top row). The structure of the gland was complete and orderly, and mucus secretion by goblet cells (red arrows) was maintained at normal levels (Figure 4A, top row). However, dnTGFβRIITLR2−/− mice had a higher colitis score (Figure 4D, $p < 0.001$). The mucosal infiltration by inflammatory cells was seen throughout the length of the colon wall and destroyed most of the glands (Figure 4A, bottom row). Due to inflammation, goblet cells could not be distinguished and mucus almost disappeared (Figure 4A, bottom row). The colon in dnTGFβRIITLR2−/− mice demonstrated crypt abscess formation (Figure 4A, bottom row). Other indicators of colitis such as changes in body weight (Figure 4B, $p < 0.001$) and colon weight (Figure 4C, $p = 0.0346$) also reflected worsening colitis in dnTGFβRIITLR2−/− mice. Thus, TLR2 deficiency caused severe colitis, structural destruction, and dysfunction of the colon.

3.4 Antibiotic treatment alleviated the exacerbated cholangitis and colitis in TLR2-deficient dnTGFβRII mice

Histopathological sections reflected that mixed antibiotic treatment alleviated inflammation in both the liver (Figure 5A) and colon (Figure 6A) of dnTGFβRIITLR2−/− mice. The portal inflammation score (Figure 5B, $p < 0.001$), bile duct damage score (Figure 5C, $p = 0.0042$), and number of liver MNCs (Figure 5D, $p = 0.0333$) were decreased after mixed antibiotic treatment. Additionally, antibiotic treatment reduced the number of upregulated T cells (Figure 5E, $p = 0.0256$), CD4+T cells (Figure 5E, $p = 0.0171$), and especially the percentage ($p = 0.0012$) and total number ($p = 0.0258$) of more active effector memory CD4+T cell subsets (CD4Tem, Figure 5F) in dnTGFβRIITLR2−/− mice. In contrast, distinct from the observation of erosion, cryptitis, crypt abscess, and transmural inflammatory infiltrate in the colon of untreated dnTGFβRIITLR2−/− mice, antibiotic-treated dnTGFβRIITLR2−/− mice demonstrated regularly arranged crypts, and inflammatory infiltrates were mild to moderate and confined to mucosa (Figure 6A). The reduced colitis score (Figure 6D, $p = 0.0250$) together with the decreased colon weight (Figure 6B, $p = 0.0424$) and increased colon length (Figure 6C, $p = 0.0403$) indicated that antibiotics alleviated the exacerbated colitis in dnTGFβRIITLR2−/− mice. Thus, eliminating intestinal bacteria resulted in significantly reduced colonic and hepatic inflammation in dnTGFβRIITLR2−/− mice.

3.5 Toll-like receptor 2 deficiency increased gut permeability and promoted gut bacterial translocation to the liver

We cultured liver homogenates of dnTGFβRIITLR2−/− mice to count the colony-forming units (CFUs). Fresh liver homogenates from wide type mice had few bacterial colonies in plates filled with Columbia Blood Agar Base (Figure 7A, 7B), while a few bacterial colonies were found in dnTGFβRII mice liver cultures (Figure 7A, 7B). However, liver CFUs of

dnTGFβRIITLR2−/− mice had changed substantially (Figure 7A) and differed by an order of magnitude (Figure 7B). As shown in Figure 7B, TLR2 deficiency in dnTGFβRII mice led to an obvious promotion of bacterial translocation to the liver, as assessed by liver culture CFUs when compared to wide type ($p = 0.0290$) and dnTGFβRII mice ($p = 0.0406$). However, antibiotics administered through drinking water to clear most of the gut microbiota could also have prevented the bacterial translocation to liver in dnTGFβRIITLR2−/− mice (Figure 7A), demonstrating reduced CFUs in liver, similar to that of the wide type controls (Figure 7B). These results suggest that the clearance of gut microbiota could prevent bacterial translocation to the liver.

To evaluate the epithelial barrier function in the TLR2-deficient PBC murine model, we first used fluorescein isothiocyanate (FITC)-dextran to analyze intestinal permeability. We observed an increased trend of gut permeability in dnTGFβRIITLR2−/− mice as compared with wide type and dnTGFβRII mice (Figure 7C). Immunofluorescence staining revealed a significant loss of zonula occludens (ZO-1) expression in the colon tissue of dnTGFβRIITLR2−/− mice (Figure 7D, bottom row), while it was normally distributed in the colon of dnTGFβRII (Figure 7D, middle row) and wide type (Figure 7D, top row) mice. Decreased ZO-1 protein expression in the colon tissue of dnTGFβRIITLR2−/− mice compared with that in the dnTGFβRII mice was confirmed by western blot (Figure 7E). These findings suggest that TLR2 deficiency disrupted the expression of epithelial tight-junction protein ZO-1 to result in increased intestinal permeability, which in turn promoted gut microbiota translocation to the liver.

4. Discussion

Altered microbiota composition and gut permeability are considered as potential causative factors in gut microbiota-induced hepatic inflammation. In our study, we report that dnTGFβRII mice manifest altered gut microbiota composition and abundance. The further disturbance of gut microbiota in these mice, by administration of a mixture of antibiotics, alleviates T-cell-mediated hepatic infiltration and bile duct damage.

To investigate how gut microbiota affected liver inflammation in this autoimmune cholangitis, we developed an epithelial-barrier-disrupted PBC murine model of TLR2-deficient dnTGFβRII mice, based on previous reports that TLR2 regulates tight-junction protein ZO-1 expression to affect intestinal epithelial barrier function [19, 31, 32]. We found that TLR2 deficiency aggravated hepatic and colonic inflammation by increasing intestinal permeability and promoting bacterial translocation to the liver in the PBC murine model. We also demonstrate that antibiotic treatment could reduce intestinal microbiota translocation to liver and alleviate hepatic pathology in TLR2-deficient mice, which further validates the important role of bacterial translocation to liver in cholangitis. Overall, our study illustrates the manner in which gut microbiota modulates liver pathology.

Gut microbiota participate in the process of digestion, help shape the mucosal immune system, and provide essential health benefits [33]. However, the microbiota also contain potential opportunistic pathogens and thus the potential to harm the host if this complex microbial community is not well balanced [34]. A key role in the maintenance of gut-liver

axis health has been attributed to intestinal homeostasis [35]. Altered composition and concentration of gut microbiota are reportedly associated with liver diseases [36]. In this study, we first demonstrate that dnTGFβRII mice exhibited a markedly diminished richness and diversity of gut microbiota. The 16S rRNA sequencing results revealed a distinct difference in the composition of gut microbiota. These findings are consistent with previous reports that dysbiosis of gut microbiota are observed in PBC patients [5].

It has been reported that antibiotic therapy could attenuate acute cholangitis in patients [37]. Also, we found that elimination of gut microbiota by antibiotic treatment significantly alleviated T-cell-mediated liver inflammation in this PBC murine model. Based on the above findings, we further addressed the mechanism by which changed gut microbiota promoted the pathogenesis of autoimmune cholangitis. We demonstrated that interruption of epithelial barrier integrity promotes the translocation of intestinal bacteria to liver and aggravates T-cell-mediated hepatic inflammation.

Toll-like receptors (TLRs) are a class of transmembrane pattern-recognition receptors that play an important role in distinct PAMPs recognition [38, 39]. Recognition and activation of TLRs could induce antimicrobial genes and regulate both innate and adaptive immune responses [40]. TLR expression on monocytes [41] in peripheral blood mononuclear cells (PBMCs) and the detection of aberrant TLR4 expression in the liver of PBC patients [42] has led to speculation that TLRs may be involved in the pathogenesis of PBC. To develop a better understanding of the role of TLRs in the pathogenesis of PBC, we also generated TLR4 knockout dnTGFβRII mice. Unlike in dnTGFβRIITLR2−/−, TLR4 deficiency had no effects on cholangitis and colitis (Figure S1, S2) in the PBC mouse model. This suggested that the role of TLR2 in this autoimmune disease is unique and different from the role of PAMPs recognition, which is the common feature of all TLRs.

TLR2 is known to play an important role in colitis by exerting effects on protecting intestinal epithelial cells to maintain epithelial barrier integrity [19, 20]. TLR2 deficiency disrupts the expression pattern of tight-junction protein ZO-1. As TLR2 modulates epithelial barrier function by regulating epithelial tight-junction integrity, we used TLR2- deficient mice as an epithelial-barrier-disrupted autoimmune cholangitis model to investigate the events occurring in the gut-liver axis. In our study, TLR2 led to increased gut permeability and decreased expression of tight-junction protein ZO-1. This alters the epithelial barrier integrity and deterioration of the intestinal environment homeostasis, which consequently promotes gut microbiota translocation to the liver. Normally, the majority of intestinal bacteria are located in the intestinal lumen and outer mucus layer. In one possible scenario, gut bacteria might breach the gut epithelium and reach the liver through the portal vein [9]. In the TLR2 knockout model, we observed significantly elevated bacterial translocation to the liver (Figure 7A, 7B). This exposes the liver to gut- derived endotoxins that activate pro-inflammatory signaling and drive inflammation. Thus, the increased bacterial translocation to the liver in the TLR2-deficient PBC murine model aggravated this autoimmune cholangitis.

In our study, although we demonstrated that gut microbiota participate in the pathogenesis of disease, we have not yet identified the specific bacteria which is/are the most pathogenic

one(s). We have examined the bacterial which are translocation to liver and cultured among liver homogenates in Figure 7A. Most abundant bacterial of them are sequenced as *E. coli* (28.6%). Since *E. coli* have the ability to induce PBC-like disease in mice [43, 44] and *E. coli* are the most prevalent bacteria isolated in women with urinary tract infection strongly association with PBC [45, 46], we presume that *E. coli* may be the pathogenic bacteria. However, since *E. coli* are common, further studies are needed. It also needs to be further investigated how the translocation of pathogenic bacteria alters liver tolerance and signaling pathways. In conclusion, using both dnTGFβRII mice and TLR2-deficient dnTGFβRII mice, we report a potentially important mechanism, namely gut microbiota driven bacterial translocation to liver, that helps explain the relationship of the microflora to liver pathology. Our study first illustrates the manner in which gut microbiota induce liver pathology in PBC and provides evidence for the role of intestinal microbiota in autoimmune liver disease, thereby shedding light on the mechanism of gut microbiota involved in the pathogenesis of human PBC.

Supplementary Material

Refer to Web version on PubMed Central for supplementary material.

Acknowledgements

We thank Yi-Fei Pei for designing the graphical abstract and Yu-Chen Wang and Tai-Dou Hu for culturing and counting the bacterial colonies of the liver homogenates.

Financial support

Financial support was provided by the Program for Guangdong Introducing Innovative and Enterpreneurial Teams (2017ZT07S054), the National Natural Science Foundation of China (81430034, 81401336, 91542123, 81671600, 81873877), the National Key R&D Program of China (2017YFA0205600), National Institutes of Health grant (DK090019), and State Key Laboratory of Pathogenesis, Prevention, Treatment of Central Asian High Incidence Diseases Fund (SKL-HIDCA-2017-6).

Abbreviations:

PBC	Primary biliary cholangitis
dnTGFβRII, TG	dominant negative transforming growth factor p receptor II
WT	wide type
TLR2	Toll-like receptor 2
TGT2	dnTGFβRII TLR2−/−
Tn	naive T cells
Tcm	central memory T cells
Tem	effector memory T cells
ABx	mixed antibiotics
HMNCs	hepatic mononuclear cells

CFUs	colony-forming units
ZO-1	zonula occludens
GAPDH	glyceraldehyde 3-phosphate dehydrogenase
DAPI	4’,6-diamidino-2-phenylindole
PAMPs	pathogen-associated molecular patterns
PBMC	peripheral blood mononuclear cell

References

[1]. Griffiths L, Dyson JK, Jones DE. The new epidemiology of primary biliary cirrhosis. Seminars in liver disease, 2014;34:318–28. [PubMed: 25057954]

[2]. Parikh-Patel A, Gold EB, Worman H, Krivy KE, Gershwin ME. Risk factors for primary biliary cirrhosis in a cohort of patients from the united states. Hepatology, 2001;33:16–21. [PubMed: 11124815]

[3]. Gershwin ME, Selmi C, Worman HJ, Gold EB, Watnik M, Utts J et al. Risk factors and comorbidities in primary biliary cirrhosis: a controlled interview-based study of 1032 patients. Hepatology, 2005;42:1194–202. [PubMed: 16250040]

[4]. Harada K, Tsuneyama K, Sudo Y, Masuda S, Nakanuma Y. Molecular identification of bacterial 16S ribosomal RNA gene in liver tissue of primary biliary cirrhosis: is Propionibacterium acnes involved in granuloma formation? Hepatology, 2001;33:530–6. [PubMed: 11230731]

[5]. Tang R, Wei Y, Li Y, Chen W, Chen H, Wang Q et al. Gut microbial profile is altered in primary biliary cholangitis and partially restored after UDCA therapy. Gut, 2017.

[6]. Crispe IN. The liver as a lymphoid organ. Annual review of immunology, 2009;27:147–63.

[7]. Volta U, Caio G, Tovoli F, De Giorgio R. Gut-liver axis: an immune link between celiac disease and primary biliary cirrhosis. Expert review of gastroenterology & hepatology, 2013;7:253–61. [PubMed: 23445234]

[8]. Henao-Mejia J, Elinav E, Thaiss CA, Licona-Limon P, Flavell RA. Role of the intestinal microbiome in liver disease. Journal of autoimmunity, 2013;46:66–73. [PubMed: 24075647]

[9]. Chassaing B, Etienne-Mesmin L, Gewirtz AT. Microbiota-liver axis in hepatic disease. Hepatology, 2014;59:328–39. [PubMed: 23703735]

[10]. Ma HD, Wang YH, Chang C, Gershwin ME, Lian ZX. The intestinal microbiota and microenvironment in liver. Autoimmunity reviews, 2015;14:183–91. [PubMed: 25315744]

[11]. Mehal WZ. The gut-liver axis: a busy two-way street. Hepatology, 2012;55:1647–9. [PubMed: 22407752]

[12]. Thomson AW, Knolle PA. Antigen-presenting cell function in the tolerogenic liver environment. Nature reviews Immunology, 2010;10:753–66.

[13]. Hartmann P, Haimerl M, Mazagova M, Brenner DA, Schnabl B. Toll-like receptor 2-mediated intestinal injury and enteric tumor necrosis factor receptor I contribute to liver fibrosis in mice. Gastroenterology, 2012;143:1330–40 e1. [PubMed: 22841787]

[14]. Qin N, Yang F, Li A, Prifti E, Chen Y, Shao L et al. Alterations of the human gut microbiome in liver cirrhosis. Nature, 2014;513:59–64. [PubMed: 25079328]

[15]. Yan AW, Fouts DE, Brandl J, Starkel P, Torralba M, Schott E et al. Enteric dysbiosis associated with a mouse model of alcoholic liver disease. Hepatology, 2011;53:96–105. [PubMed: 21254165]

[16]. Yuksel M, Wang Y, Tai N, Peng J, Guo J, Beland K et al. A novel “humanized mouse” model for autoimmune hepatitis and the association of gut microbiota with liver inflammation. Hepatology, 2015;62:1536–50. [PubMed: 26185095]

[17]. Sabino J, Vieira-Silva S, Machiels K, Joossens M, Falony G, Ballet V et al. Primary sclerosing cholangitis is characterised by intestinal dysbiosis independent from IBD. Gut, 2016;65:1681–9. [PubMed: 27207975]

[18]. Kummen M, Holm K, Anmarkrud JA, Nygard S, Vesterhus M, Hoivik ML et al. The gut microbial profile in patients with primary sclerosing cholangitis is distinct from patients with ulcerative colitis without biliary disease and healthy controls. Gut, 2017;66:611–9. [PubMed: 26887816]

[19]. Cario E, Gerken G, Podolsky DK. Toll-like receptor 2 controls mucosal inflammation by regulating epithelial barrier function. Gastroenterology, 2007;132:1359–74. [PubMed: 17408640]

[20]. Brun P, Giron MC, Qesari M, Porzionato A, Caputi V, Zoppellaro C et al. Toll-like receptor 2 regulates intestinal inflammation by controlling integrity of the enteric nervous system. Gastroenterology, 2013;145:1323–33. [PubMed: 23994200]

[21]. Gorelik L, Flavell RA. Abrogation of TGFbeta signaling in T cells leads to spontaneous T cell differentiation and autoimmune disease. Immunity, 2000;12:171–81. [PubMed: 10714683]

[22]. Oertelt S, Lian ZX, Cheng CM, Chuang YH, Padgett KA, He XS et al. Anti-mitochondrial antibodies and primary biliary cirrhosis in TGF-beta receptor II dominant-negative mice. Journal of immunology, 2006;177:1655–60.

[23]. Caricilli AM, Picardi PK, de Abreu LL, Ueno M, Prada PO, Ropelle ER et al. Gut microbiota is a key modulator of insulin resistance in TLR 2 knockout mice. PLoS biology, 2011;9:e1001212. [PubMed: 22162948]

[24]. Yurkovetskiy L, Burrows M, Khan AA, Graham L, Volchkov P, Becker L et al. Gender bias in autoimmunity is influenced by microbiota. Immunity, 2013;39:400–12. [PubMed: 23973225]

[25]. Meyer F, Paarmann D, D'Souza M, Olson R, Glass EM, Kubal M et al. The metagenomics RAST server - a public resource for the automatic phylogenetic and functional analysis of metagenomes. BMC bioinformatics, 2008;9:386. [PubMed: 18803844]

[26]. Edgar RC. UPARSE: highly accurate OTU sequences from microbial amplicon reads. Nature methods, 2013;10:996–8. [PubMed: 23955772]

[27]. Ando Y, Yang GX, Tsuda M, Kawata K, Zhang W, Nakajima T et al. The immunobiology of colitis and cholangitis in interleukin-23p19 and interleukin-17A deleted dominant negative form of transforming growth factor beta receptor type II mice. Hepatology, 2012;56:1418–26. [PubMed: 22532156]

[28]. Lian ZX, Okada T, He XS, Kita H, Liu YJ, Ansari AA et al. Heterogeneity of dendritic cells in the mouse liver: identification and characterization of four distinct populations. Journal of immunology, 2003;170:2323–30.

[29]. Wang YC, Ma HD, Yin XY, Wang YH, Liu QZ, Yang JB et al. Forkhead Box O1 Regulates Macrophage Polarization Following Staphylococcus aureus Infection: Experimental Murine Data and Review of the Literature. Clin Rev Allergy Immunol, 2016;51:353–69. [PubMed: 26924010]

[30]. Cani PD, Bibiloni R, Knauf C, Waget A, Neyrinck AM, Delzenne NM et al. Changes in gut microbiota control metabolic endotoxemia-induced inflammation in high-fat diet-induced obesity and diabetes in mice. Diabetes, 2008;57:1470–81. [PubMed: 18305141]

[31]. Cario E, Gerken G, Podolsky DK. Toll-like receptor 2 enhances ZO-1-associated intestinal epithelial barrier integrity via protein kinase C. Gastroenterology, 2004;127:224–38. [PubMed: 15236188]

[32]. Cario E Barrier-protective function of intestinal epithelial Toll-like receptor 2. Mucosal immunology, 2008;1 Suppl 1:S62–6. [PubMed: 19079234]

[33]. Robinson CJ, Bohannan BJ, Young VB. From structure to function: the ecology of host-associated microbial communities. Microbiology and molecular biology reviews : MMBR, 2010;74:453–76. [PubMed: 20805407]

[34]. Hooper LV, Macpherson AJ. Immune adaptations that maintain homeostasis with the intestinal microbiota. Nature reviews Immunology, 2010;10:159–69.

[35]. Compare D, Coccoli P, Rocco A, Nardone OM, De Maria S, Carteni M et al. Gut--liver axis: the impact of gut microbiota on non alcoholic fatty liver disease. Nutrition, metabolism, and cardiovascular diseases : NMCD, 2012;22:471–6.

[36]. Miyake Y, Yamamoto K. Role of gut microbiota in liver diseases. Hepatol Res, 2013;43:139–46. [PubMed: 22970713]

[37]. Mosler P Management of acute cholangitis. Gastroenterology & hepatology, 2011;7:121–3. [PubMed: 21475420]

[38]. Akira S, Uematsu S, Takeuchi O. Pathogen recognition and innate immunity. Cell, 2006;124:783–801. [PubMed: 16497588]

[39]. Seki E, Brenner DA. Toll-like receptors and adaptor molecules in liver disease: update. Hepatology, 2008;48:322–35. [PubMed: 18506843]

[40]. Hooper LV, Wong MH, Thelin A, Hansson L, Falk PG, Gordon JI. Molecular analysis of commensal host- microbial relationships in the intestine. Science, 2001;291:881–4. [PubMed: 11157169]

[41]. Mao TK, Lian ZX, Selmi C, Ichiki Y, Ashwood P, Ansari AA et al. Altered monocyte responses to defined TLR ligands in patients with primary biliary cirrhosis. Hepatology, 2005;42:802–8. [PubMed: 16175622]

[42]. Wang AP, Migita K, Ito M, Takii Y, Daikoku M, Yokoyama T et al. Hepatic expression of toll-like receptor 4 in primary biliary cirrhosis. Journal of autoimmunity, 2005;25:85–91. [PubMed: 16006099]

[43]. Koutsoumpas AL, Smyk DS, Bogdanos DP. E. coli Induced Experimental Model of Primary Biliary Cirrhosis: At Last. International journal of hepatology, 2014;2014:848373. [PubMed: 25580301]

[44]. Wang JJ, Yang GX, Zhang WC, Lu L, Tsuneyama K, Kronenberg M et al. Escherichia coli infection induces autoimmune cholangitis and anti-mitochondrial antibodies in non-obese diabetic (NOD).B6 (Idd10/Idd18) mice. Clinical and experimental immunology, 2014;175:192–201. [PubMed: 24128311]

[45]. Smyk DS, Bogdanos DP, Kriese S, Billinis C, Burroughs AK, Rigopoulou EI. Urinary tract infection as a risk factor for autoimmune liver disease: from bench to bedside. Clinics and research in hepatology and gastroenterology, 2012;36:110–21. [PubMed: 21907008]

[46]. Cusumano CK, Pinkner JS, Han Z, Greene SE, Ford BA, Crowley JR et al. Treatment and prevention of urinary tract infection with orally active FimH inhibitors. Science translational medicine, 2011;3:109ra15.

Highlights:

- Dysbiosis of gut microbiota contributes to autoimmune cholangitis
- Disrupted epithelial barrier aggravated cholangitis in dnTGFβRII mice
- TLR2 deficiency aggravated colitis and colon injury in dnTGβRII mice
- Antibiotic treatment alleviated the exacerbated cholangitis and colitis
- TLR2 deficiency increased gut permeability and promoted gut bacterial translocation

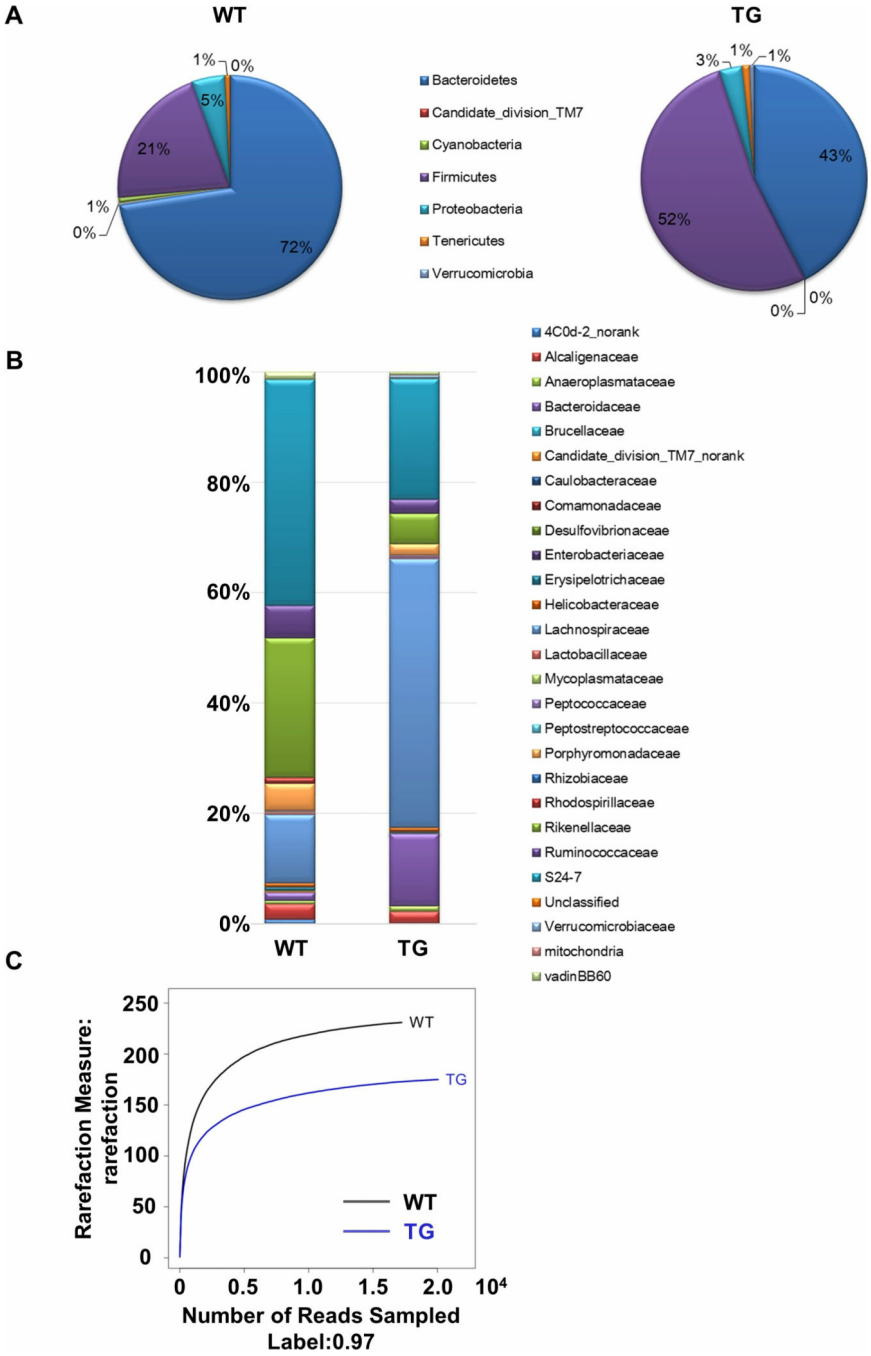

Figure 1. dnTGFβRII mice exhibited taxonomical alterations and species richness reduction in gut microbiota.

454 pyrosequencing analysis of the fecal microbiota composition from WT and TG mice at both the (A) phylum and (B) family level. (C) Rarefaction curve showing the changes between WT and TG mice with respect to microbiota richness.

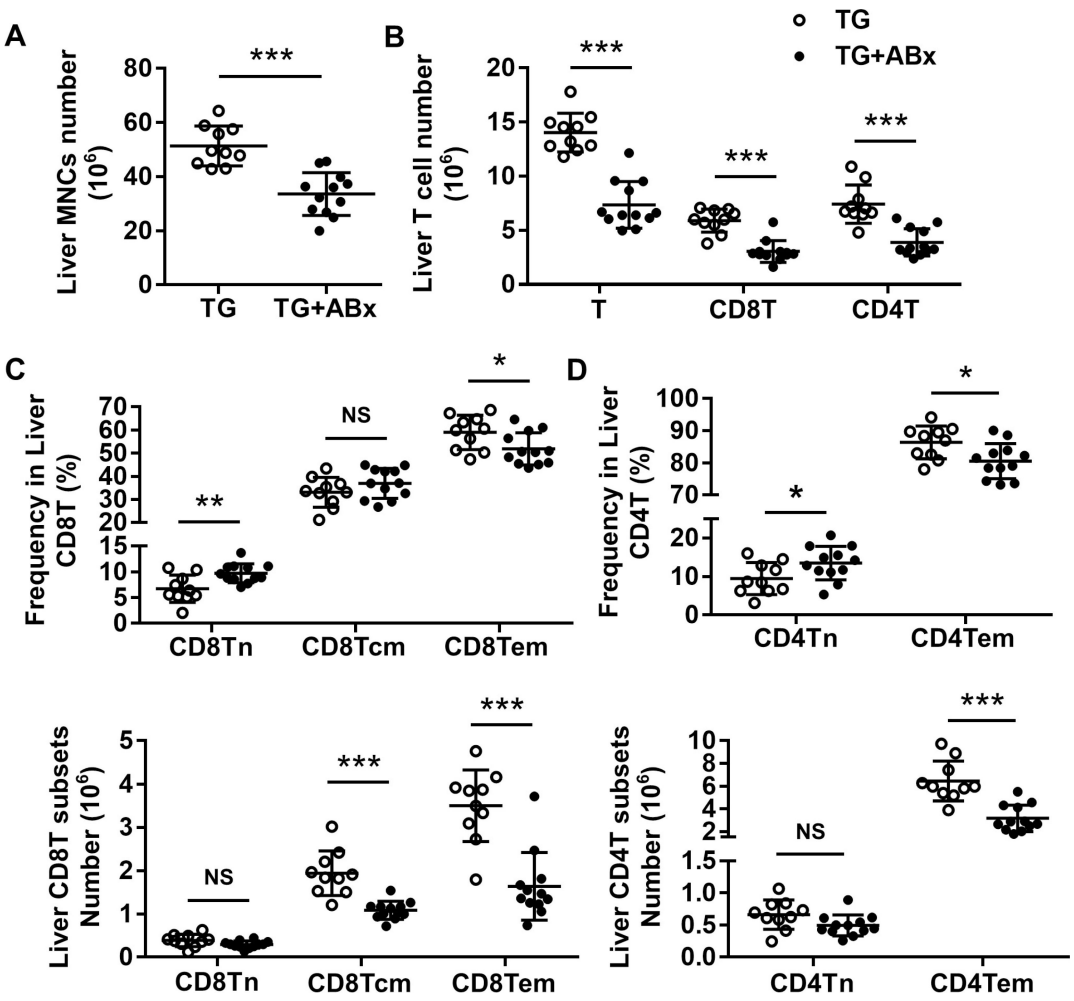

Figure 2. Antibiotic treatment alleviated hepatic T-cell-mediated infiltration in dnTGFβRII mice

(A) Absolute number of hepatic mononuclear cells from dnTGFβRII mice (TG; n=10) and dnTGFβRII mice with mixed antibiotics treatment (TG+ABx; n=12). (B) Cell numbers of total T cells and CD8+T and CD4+T cell subsets in the liver of TG (n=10) and TG+ABx (n=12) mice, as determined by flow cytometry. Frequency (above) and absolute number (below) of (C) CD8Tn, CD8Tcm, and CD8Tem; as well as (D) CD4Tn and CD4Tem cell subsets in the liver of TG (n=10) and TG+ABx (n=12) mice. Data are presented as mean ± SD. *p<0.05, **p<0.01, ***p<0.001.

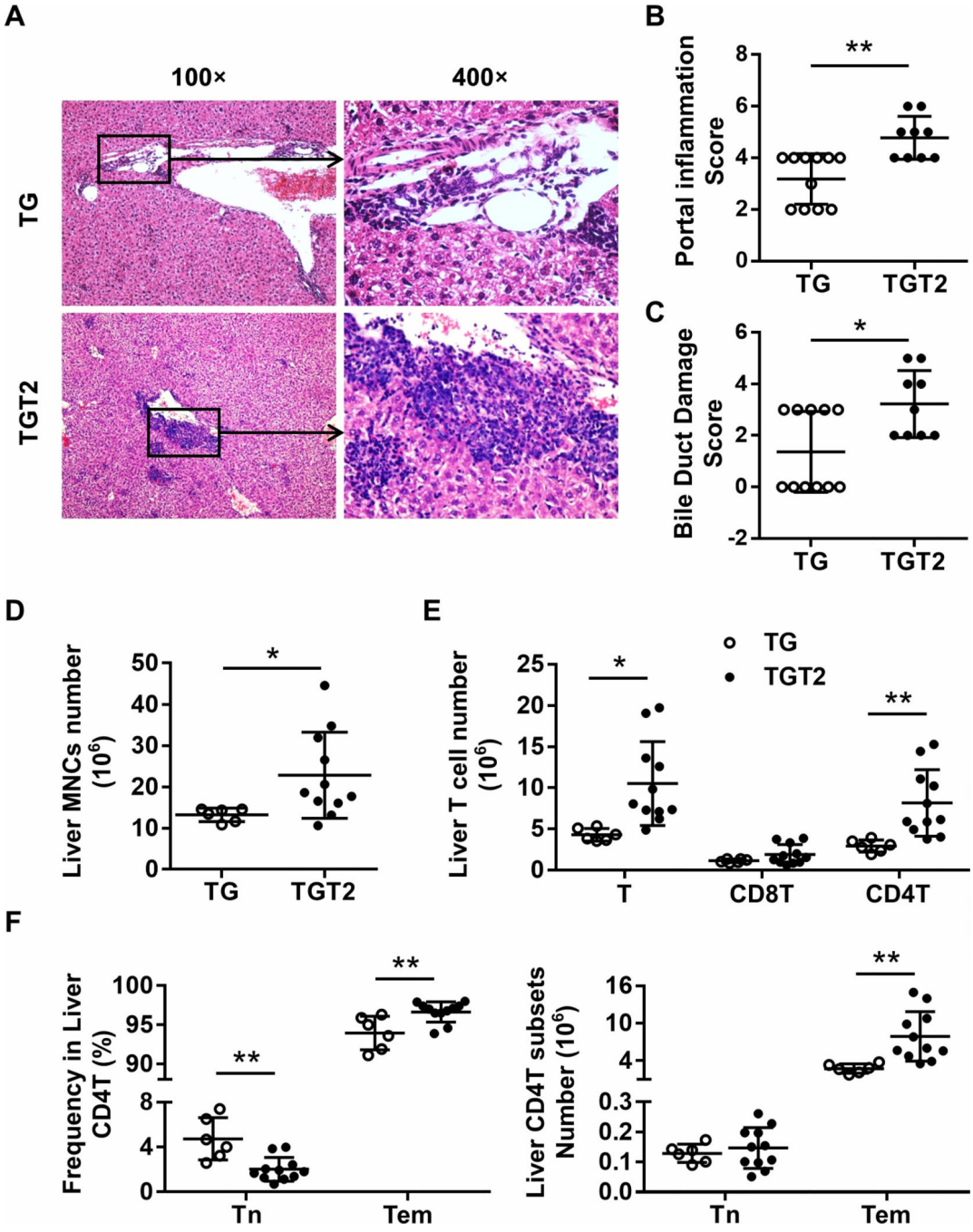

Figure 3. Toll-like receptor 2 deficiency aggravated hepatic T-cell-mediated cholangitis in dnTGFβRII mice

(A) Representative H&E staining of liver sections of female dnTGFβRII (TG) and dnTGFβRII TLR2−/− (TGT2) mice at 13–14 weeks of age. (B) Scores of portal inflammation in TG (n=11) and TGT2 (n=9) mice. (C) Scores of bile duct damage in TG (*n*=11) and TGT2 mice (*n*=9). (D) Absolute number of hepatic mononuclear cells from TG (*n*=6) and TGT2 (*n*=11) mice. (E) Cell numbers of total T cells and CD8+T and CD4+T cell subsets in the liver of TG (*n*=6) and TGT2 (*n*=11) mice analyzed by flow cytometry. (F) Frequency (left) and absolute number (right) of naive CD4+T (CD44-CD62L+) and effector

memory CD4+T (CD44+CD62L-) cell subsets in the liver of TG (n=6) and TGT2 (n=11) mice. Data are presented as mean ± SD. *p<0.05, **p<0.01.

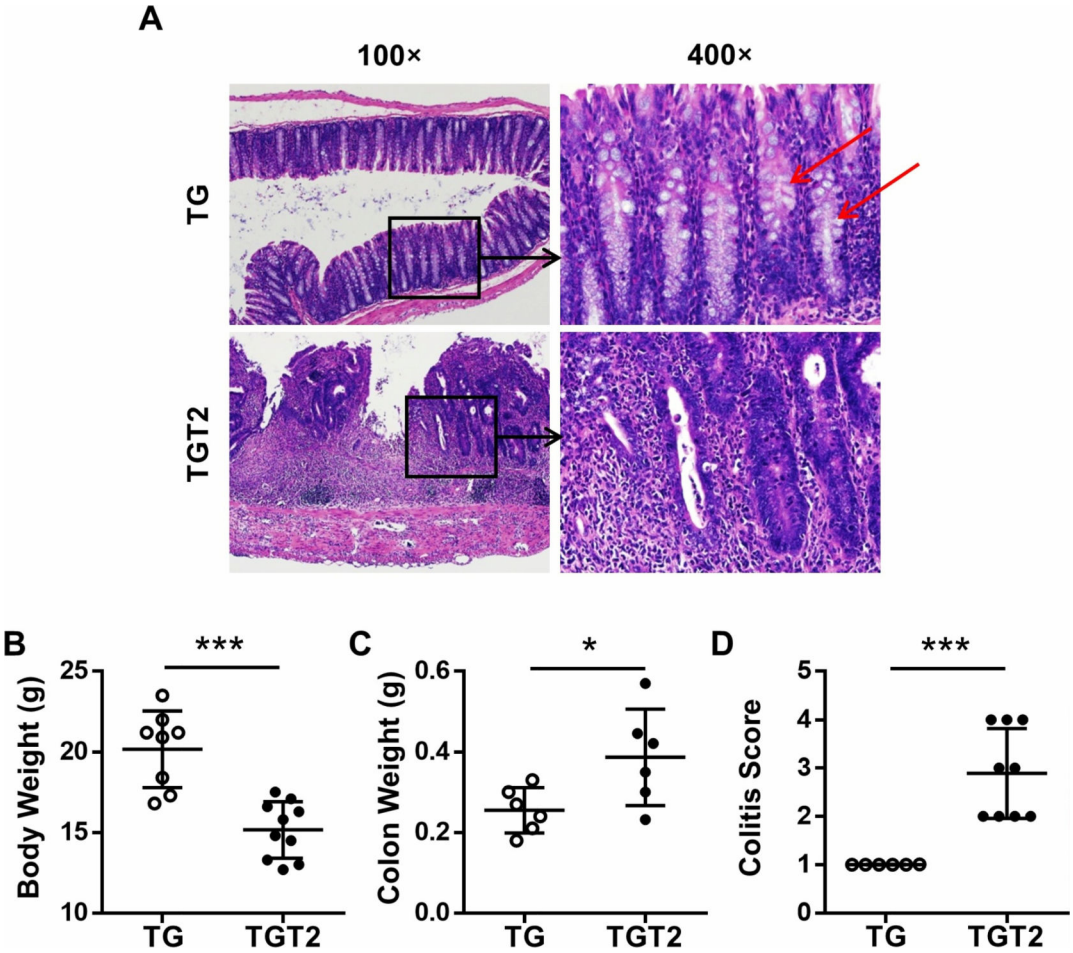

Figure 4. Toll-like receptor 2 deficiency aggravated colitis in dnTGFβRII mice

(A) Representative H&E staining of colon section of female TG and TGT2 mice at 13–14 weeks of age. (B) Body weight of TG (n=8) and TGT2 (n=10) mice. (C) Colon weight of TG (n=6) and TGT2 (n=6) mice. (D) Scores of colitis in TG (n=6) and TGT2 (n=9) mice. Data are presented as mean ± SD. *p<0.05, ***p<0.001.

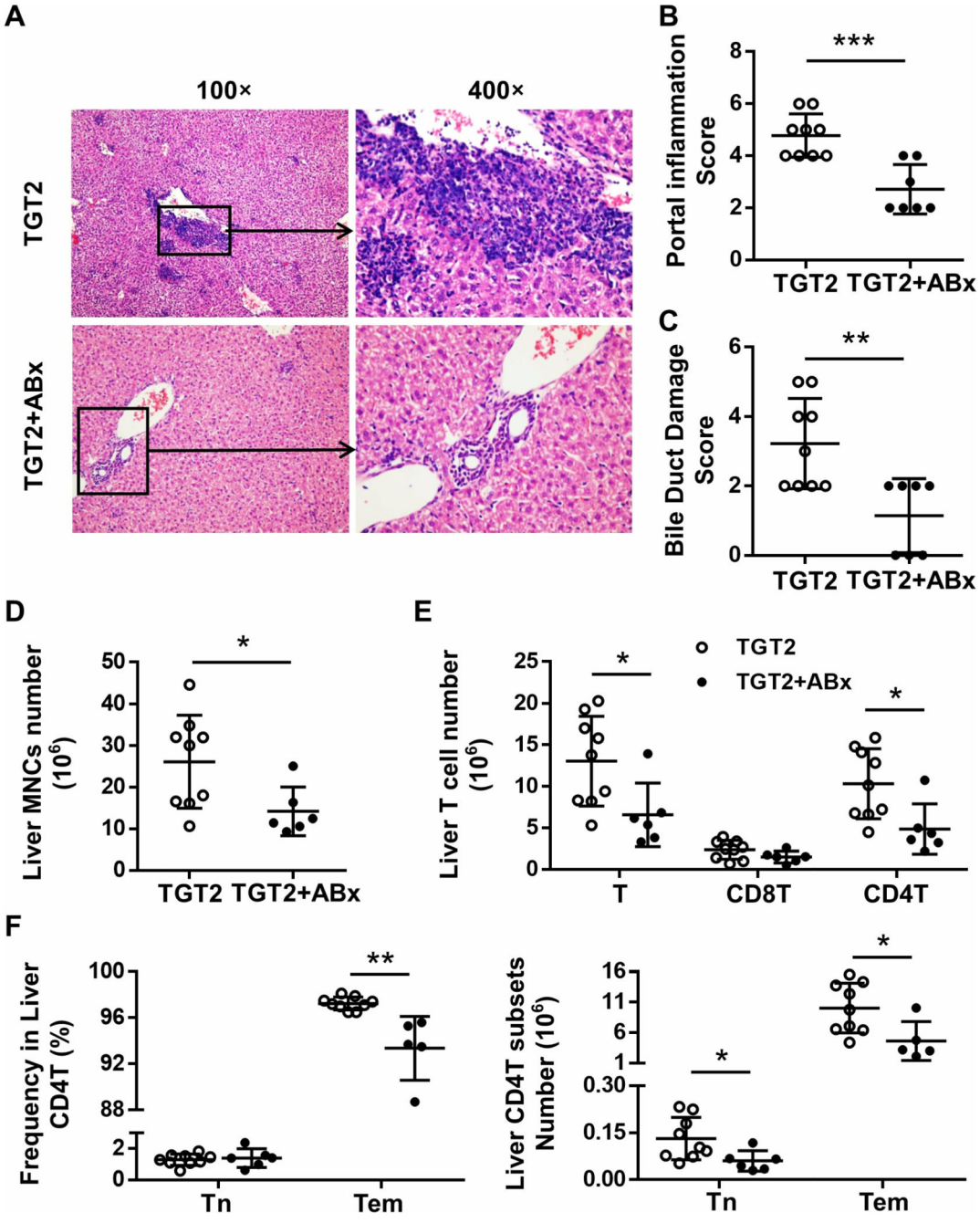

Figure 5. Antibiotic treatment alleviated exacerbated cholangitis in dnTGFβRII TLR2−/− mice

(A) Representative H&E staining of liver sections of 13–14-week-old female TGT2 mice with (TGT2+ABx) or without (TGT2) mixed antibiotics treatment. (B) Scores of portal inflammation in TGT2 (n=9) and TGT2+ABx mice (n=7). (C) Scores of bile duct damage in TGT2 (n=9) and TGT2+ABx mice (n=7). (D) Absolute number of hepatic mononuclear cells from TGT2 (n=9) and TGT2+ABx mice (n=6). (E) Cell numbers of total T cells and CD8+T and CD4+T cell subsets in the liver of TGT2 (n=9) and TGT2+ABx (n=6) mice, as determined by flow cytometry. (F) Frequency (left) and absolute number (right) of naive CD4+T (CD44-CD62L+) and effector memory CD4+T (CD44+CD62L-) cell subsets in the

liver of TGT2 (n=9) and TGT2+ABx (n=6) mice. Data are presented as mean ± SD. *p<0.05, **p<0.01, ***p<0.001.

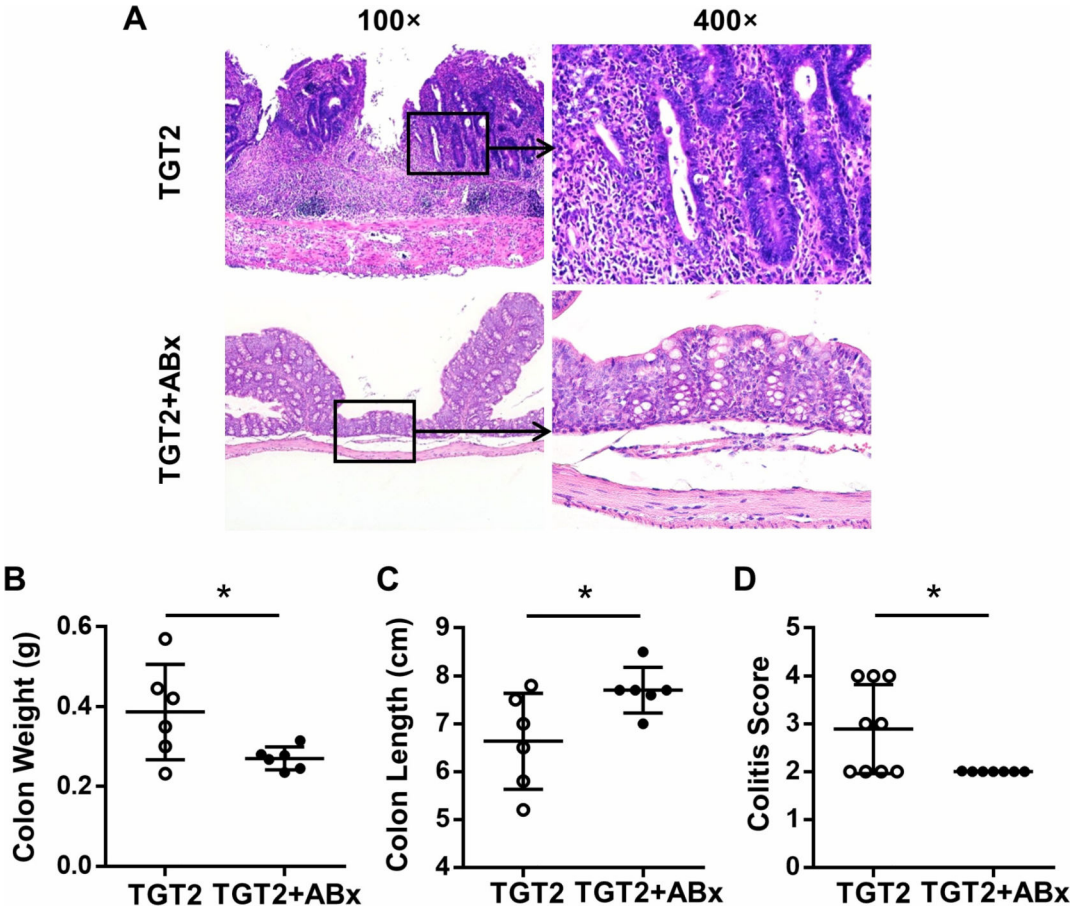

Figure 6. Antibiotic treatment alleviates exacerbated colitis in dnTGFβRII TLR2−/− mice

(A) Representative H&E staining of colon section of 13–14-week-old female TGT2 mice without (TGT2) or with (TGT2+ABx) mixed antibiotics treatment. (B) Colon weight of TGT2 (n=6) and TGT2+ABx (n=6) mice. (C) Colon length of TGT2 (n=6) and TGT2+ABx (n=6) mice. (D) Scores of colitis in TGT2 (n=9) and TGT2+ABx (n=7) mice. Data are presented as mean ± SD. *p<0.05.

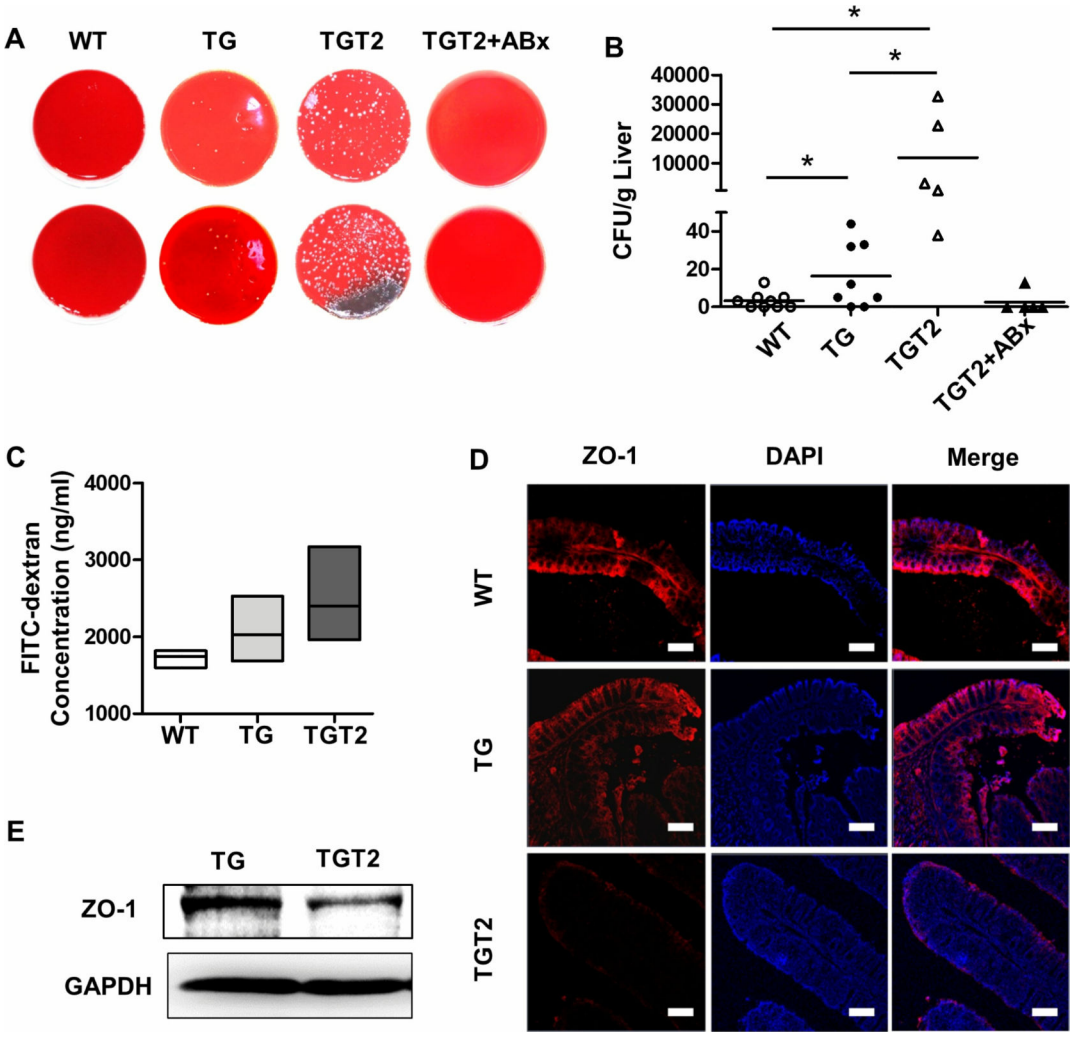

Figure 7. Toll-like receptor 2 deficiency increased gut permeability and promoted bacterial translocation to the liver

(A) Fresh livers isolated from WT (*n*=9), TG (*n*=8), TGT2 (*n*=5), and TGT2+ABx (*n*=5) mice were homogenized and plated on Columbia Blood Agar Base. After 24-h incubation, the CFUs were counted and calculated as count per gram weight of the livers (B). (C) Intestinal permeability was measured by determining the concentration of FITC-dextran in the serum of WT (*n*=3), TG (*n*=3), and TGT2 (*n*=4) mice. (D) Representative immunofluorescence staining of frozen colon tissues from WT, TG, and TGT2 mice. Sections labeled with anti-ZO-1 (red, left column) and DAPI (blue, middle column) and merged images (right column) are shown (100*, scale bars: 100 μm). (E) Immunoblotting analysis for ZO-1 (194 kDa) in colon homogenates of TG and TGT2 mice. GAPDH (36 kDa) served as reference. Data are presented as mean ± SD. *p<0.05.